Longitudinal Dispersion Coefficient in Single-Channel Streams

Z.-Q. Deng[1]; L. Bengtsson, F.ASCE[2]; V. P. Singh, F.ASCE[3]; and D. D. Adrian, F.ASCE[4]

Abstract: Using a new channel shape equation for straight channels and a more versatile channel shape or local flow depth equation for natural streams a method is developed for prediction of the longitudinal dispersion coefficient in single-channel natural streams, including straight and meandering ones. The method involves derivation of a new triple integral expression for the longitudinal dispersion coefficient and development of an analytical method for prediction of this coefficient in natural streams. The proposed method is verified using 70 sets of field data collected from 30 streams in the United States ranging from straight manmade canals to sinuous natural rivers. The new method predicts the longitudinal dispersion coefficient, where more than 90% calculated values range from 0.5 to 2 times the observed values. The advantage of the new method is that it is capable of accurately predicting the longitudinal dispersion coefficient in single-channel natural streams without using detailed dye concentration test data. A comparison between the new method and the existing methods shows that the new method significantly improves the prediction of the longitudinal dispersion coefficient.

DOI: 10.1061/(ASCE)0733-9429(2002)128:10(901)

CE Database keywords: Wave dispersion; Streams; Channel flow; Coefficients.

Introduction

River pollution has received much attention in recent years. The longitudinal dispersion coefficient is a fundamental parameter in hydraulic modeling of river pollution, for it is a measure of the intensity of the mixing of pollutants in natural streams and is, therefore, of great interest to river managers, environmental engineers, institutional researchers, among others, who are involved in river water pollution control.

More than 30 years ago Fischer (1967) developed a theory for determination of the longitudinal dispersion coefficient from cross-sectional data and the transverse mixing coefficient. However, predicted longitudinal dispersion coefficients often deviate from observed ones by orders of magnitude. The deviation is attributed mainly to the inability to account for meandering and other nonuniform conditions of the river.

The overall objective of this paper is to develop a simple yet reliable method of estimating the longitudinal dispersion coefficient in single-channel natural streams, including straight and meandering ones. The method employs bulk channel parameters, which are easily available without dye experiments. The specific objectives are therefore to: (1) establish a local flow depth equation describing the cross-sectional channel shape of natural streams by incorporating the channel sinuosity; (2) derive a new triple integral expression defining the longitudinal dispersion coefficient; and (3) determine the parameters of the new method easily and develop a simple and accurate solution for obtaining the longitudinal dispersion coefficient.

Previous Investigations

Numerous investigators have contributed to the understanding of the mechanisms of longitudinal dispersion in rivers, beginning with the simplest dispersion of dissolved contaminants in laminar pipe flow (Taylor 1953) to turbulent pipe flow (Taylor 1954). Elder (1959) extended the dispersion in pipe to the mixing in an infinitely wide channel of constant depth and proposed that the governing mechanism for dispersion in a wide channel is the vertical velocity gradient. Fischer (1967) attributed the lateral velocity heterogeneity to the underlying mechanism of longitudinal dispersion. McCutcheon (1989) summarized studies related to longitudinal dispersion. Despite the pioneering work of Taylor and the landmark contribution of Fischer, and seminal studies of Elder (1959); Sooky (1969); Chatwin (1971); Czernuszenko (1990); and Rutherford (1994) among others, the discrepancies between the magnitudes of the observed and predicted longitudinal dispersion coefficients are still found in the range of 1–3 orders of magnitude and existing methods, in general, underestimate the dispersion coefficient (Sooky 1969; Godfrey and Frederick 1970; Chatwin 1971; Nordin and Sabol 1974; Liu 1977; Seo and Cheong 1998). Such substantial discrepancies are often attributed to the irregularity, spiral flow, and the storage in dead zones in natural streams.

Using a spectral technique, a stochastic method was proposed to estimate an effective longitudinal dispersion coefficient, which included the impact of irregular variations in the river width and bed elevation, and concluded that the effective longitudinal dispersion coefficient could be ten or more times higher than the

[1]Associate Professor, Dept. of Civil Engineering, Shihezi Univ., Shihezi, Xinjiang 832003, P.R. China.

[2]Professor, Dept. of Water Resources Engineering, Lund Univ., Box 118, S-22100 Lund, Sweden.

[3]A. K. Barton Professor, Dept. of Civil & Environmental Engineering, Louisiana State Univ., Baton Rouge, LA 70803-6405.

[4]Rubicon Professor, Dept. of Civil & Environmental Engineering, Louisiana State Univ., Baton Rouge, LA 70803-6405. E-mail: dadrian@lsu.edu

Note. Discussion open until March 1, 2003. Separate discussions must be submitted for individual papers. To extend the closing date by one month, a written request must be filed with the ASCE Managing Editor. The manuscript for this paper was submitted for review and possible publication on August 23, 2001; approved on April 19, 2002. This paper is part of the ***Journal of Hydraulic Engineering***, Vol. 128, No. 10, October 1, 2002. ©ASCE, ISSN 0733-9429/2002/10-901–916/$8.00+$.50 per page.

longitudinal dispersion coefficient of a corresponding straight channel. Fischer (1969) explained the considerable discrepancies by considering the effect of variation of the cross-sectional geometry on dispersion along the course of natural streams and pointed out that stream meanders influence longitudinal dispersion in two ways. First, the concentration of high velocities on the outside of river bends results in increased dispersion. Second, river bends induce secondary currents and therefore increased transverse mixing, which means that the concentration of a pollutant tends to be more uniform in a cross section, and thus reduces the longitudinal dispersion. To obtain a mean dispersion coefficient of a meandering stream, Fischer (1969) suggested that individual dispersion coefficients should be determined from some typical channel geometries and velocity distributions at various cross sections of a stream, and an average longitudinal dispersion coefficient be determined. Although the discrepancies were not reduced significantly, Fischer's suggestions are instructive.

Along a meandering stream there are dead zones, where the water is rather isolated from the running water in the main channel. The water exchange between the running water in the main channel and the more or less still water in these dead zones influences the mixing along the stream. There are multiparameter models for computing this water exchange and the related longitudinal dispersion (Bencala and Walters 1983; Czernuszenko and Rowinski 1997, 1998; Lees et al. 2000; Wörman 2000; Fernald et al. 2001). Seo and Cheong (2001) solved a four-parameter dead zone model by using the moment matching method and stated that the concentration curves calculated from the four parameter-model fit observed concentration curves better than the existing methods. The majority of the dead-zone models seem capable of providing good predictions of the dispersion process in natural rivers, if there is a large number of detailed dye test measurements for determining the parameters involved in the dead zone equations. A high-resolution numerical method can satisfactorily predict the longitudinal and lateral dispersion in natural streams with arbitrary geometry and bathymetry, provided the detailed field concentration measurements are made at strategically placed monitoring stations (Piasecki and Katopodes 1999).

It follows from the above discussion that existing methods of predicting the dispersion process in natural rivers require detailed dye test concentration data. Such a requirement limits the application of advanced methods, because detailed concentration data are not readily available in most natural streams due to the high cost associated with such measurements. Consequently, it is necessary for effective river pollution control that an accurate analytical method for predicting the longitudinal dispersion coefficient in natural streams is developed, a method which does not require detailed dye test concentration data.

Theoretical Formulation

In order to clarify the concept of diffusion and dispersion and to derive an analytical equation of the longitudinal dispersion coefficient for natural streams including straight and meandering ones, it is necessary to consider the origin of diffusion and dispersion. If there are no sources/sinks, the three-dimensional constituent transport equation in natural streams can be written in terms of instantaneous variables as (Martin and McCutcheon 1999)

$$\frac{\partial c}{\partial t}+\frac{\partial(uc)}{\partial s}+\frac{\partial(\nu c)}{\partial \eta}+\frac{\partial(wc)}{\partial z}=D_m\left(\frac{\partial^2 c}{\partial s^2}+\frac{\partial^2 c}{\partial \eta^2}+\frac{\partial^2 c}{\partial z^2}\right) \quad (1)$$

where t = time; s, η, and z = coordinates along longitudinal, lateral, and vertical directions in the natural coordinate system, respectively; u, υ, and w = flow velocities along the three coordinate directions in LT^{-1}; c = constituent concentration in L^3L^{-3}; u, υ, w, and c = instantaneous values; and D_m = coefficient of molecular diffusion in L^2T^{-1}. Although the instantaneous velocities u, υ, and w of river flow can be obtained by means of advanced flow measurement instruments, it is convenient to represent the instantaneous values u, υ, and w in terms of the time-averaged values (for a specified flow condition) $\bar{u}$, $\bar{\upsilon}$, and $\bar{w}$ and the turbulent fluctuating values u', υ', and w' of turbulent flow, i.e., $u=\bar{u}+u'$, $\upsilon=\bar{\upsilon}+\upsilon'$, $w=\bar{w}+w'$, and $c=\bar{c}+c'$. Substituting these replacements of u, υ, w, and c into Eq. (1) and integrating the equation with respect to time t, one gets

$$\frac{\partial \bar{c}}{\partial t}+\frac{\partial(\bar{u}\bar{c})}{\partial s}+\frac{\partial(\bar{\upsilon}\bar{c})}{\partial \eta}+\frac{\partial(\bar{w}\bar{c})}{\partial z}=D_m\left(\frac{\partial^2 \bar{c}}{\partial s^2}+\frac{\partial^2 \bar{c}}{\partial \eta^2}+\frac{\partial^2 \bar{c}}{\partial z^2}\right)-\frac{\partial(\overline{u'c'})}{\partial s}-\frac{\partial(\overline{\upsilon'c'})}{\partial \eta}-\frac{\partial(\overline{w'c'})}{\partial z} \quad (2)$$

The overbars indicate the time-averaged values of the quantities under the bar, and u', υ', w', and c' = fluctuations about the mean values. By definition, the average of the fluctuating terms must be zero. The last three terms on the right-hand side of Eq. (2) represent the transport associated with the turbulent fluctuations and are generally assumed to be proportional to the gradient of $\bar{c}$ on the basis of experimental results (Holley 1969; McCutcheon 1989; Martin and McCutcheon 1999)

$$-\overline{u'c'}=E_s\frac{\partial \bar{c}}{\partial s}, \quad -\overline{\upsilon'c'}=E_\eta\frac{\partial \bar{c}}{\partial \eta},$$

and

$$-\overline{w'c'}=E_z\frac{\partial \bar{c}}{\partial z} \quad (3)$$

in which E_s, E_η, and E_z = turbulent diffusion coefficients of flow along the direction s, η, and z, respectively, due to the time averaging of integration. Except at the interfaces where there are no turbulent eddies, the role of molecular diffusion is negligible as compared to that of turbulent diffusion in constituent transport (McCutcheon 1989). Substitution of Eq. (3) into Eq. (2) yields

$$\frac{\partial \bar{c}}{\partial t}+\frac{\partial(\bar{u}\bar{c})}{\partial s}+\frac{\partial(\bar{\upsilon}\bar{c})}{\partial \eta}+\frac{\partial(\bar{w}\bar{c})}{\partial z}=\frac{\partial}{\partial s}\left((D_m+E_s)\frac{\partial \bar{c}}{\partial s}\right)+\frac{\partial}{\partial \eta}\left((D_m+E_\eta)\frac{\partial \bar{c}}{\partial \eta}\right)+\frac{\partial}{\partial z}\left((D_m+E_z)\frac{\partial \bar{c}}{\partial z}\right) \quad (4)$$

All the time-averaged quantities in Eq. (4) can be expressed in the form of the depth-averaged quantities as long as the mixing process over the full flow depth is accomplished, i.e., $\bar{u}=\bar{\bar{u}}+u''$, $\bar{\upsilon}=\bar{\bar{\upsilon}}+\upsilon''$, $\bar{w}=\bar{\bar{w}}+w''$, and $\bar{c}=\bar{\bar{c}}+c''$. $\bar{\bar{u}}$, $\bar{\bar{\upsilon}}$, and $\bar{\bar{w}}$ = depth-averaged velocities; and u'', υ'' and w'' = deviations from $\bar{u}$, $\bar{\upsilon}$, and $\bar{w}$. Similarly, $\bar{\bar{c}}$ = depth-averaged concentration; and c'' = deviation of $\bar{c}$ from $\bar{\bar{c}}$. Inserting these depth-averaged quantities into Eq. (4) and integrating the equation over local flow depth h by using Leibnitz's rule leads to (Appendix I)

$$h\left(\frac{\partial \bar{c}}{\partial t}+\frac{\partial(\bar{u}\bar{c})}{\partial s}+\frac{\partial(\bar{v}\bar{c})}{\partial \eta}\right)=\frac{\partial}{\partial s}\left(h(D_m+E_s)\frac{\partial \bar{c}}{\partial s}\right)+\frac{\partial}{\partial \eta}\left(h(D_m+E_\eta)\frac{\partial \bar{c}}{\partial \eta}\right)-\frac{\partial h(\overline{u''c''})}{\partial s}-\frac{\partial h(\overline{v''c''})}{\partial \eta} \quad (5)$$

where it has been considered that the turbulent diffusion coefficients E_s and E_η are constant at the boundaries. The molecular diffusion coefficient D_m related terms ($D_m\partial c/\partial s$ and $D_m\partial c/\partial \eta$) are small at the water surface and the terms appearing according to the Leibnitz rule when integrating the first two terms on the right-hand side can be neglected (Appendix I). In the same manner as Eq. (3), expressions for the cross products of the fluctuating terms in Eq. (5) are developed using an analogy to molecular diffusion as

$$-\overline{u''c''}=K_{sz}\frac{\partial \bar{c}}{\partial s}$$
$$-\overline{v''c''}=K_{\eta z}\frac{\partial \bar{c}}{\partial \eta} \quad (6)$$

where K_{sz} and $K_{\eta z}$ = dispersion coefficients in the s and η directions due to the vertical gradients of velocity and concentration. The last two terms of Eq. (5) denote the shear contribution to the dispersion.

Although they are similar in form, Eqs. (6) and (3) are different by nature. K_{sz} and $K_{\eta z}$ stem from the vertical velocity and concentration gradients and thus from the deviation of the longitudinal and lateral velocities from their depth-averaged values, whereas E_s, E_η, and E_z originate from the turbulent eddies and thus from the deviation of the longitudinal, lateral, and vertical instantaneous velocities from their time-averaged values. The eddy turbulence at small scales is the predominant mechanism in the turbulent diffusion process, and the velocity variation in the cross section is the predominant mechanism in the longitudinal dispersion process. Such an understanding of the dispersion mechanism is essential for the determination of an accurate expression defining the dispersion coefficient. Substituting Eq. (6) into Eq. (5) results in

$$h\left(\frac{\partial \bar{c}}{\partial t}+\frac{\partial(\bar{u}\bar{c})}{\partial s}+\frac{\partial(\bar{v}\bar{c})}{\partial \eta}\right)=\frac{\partial}{\partial s}\left(h(D_m+E_s+K_{sz})\frac{\partial \bar{c}}{\partial s}\right)+\frac{\partial}{\partial \eta}\left(h(D_m+E_\eta+K_{\eta z})\frac{\partial \bar{c}}{\partial \eta}\right) \quad (7)$$

The different dispersion coefficients D_m for molecular diffusion, E for turbulent diffusion, and K for advective dispersion, can be lumped together to form mixing coefficients M, being different in s and η directions. Dividing both sides of Eq. (7) by h gives

$$\frac{\partial \bar{c}}{\partial t}+\frac{\partial(\bar{u}\bar{c})}{\partial s}+\frac{\partial(\bar{v}\bar{c})}{\partial \eta}=\frac{1}{h}\frac{\partial}{\partial s}\left(hM_s\frac{\partial \bar{c}}{\partial s}\right)+\frac{1}{h}\frac{\partial}{\partial \eta}\left(hM_\eta\frac{\partial \bar{c}}{\partial \eta}\right) \quad (8a)$$

in which the transverse mixing coefficient M_η and the longitudinal mixing coefficient M_s are

$$M_\eta=D_m+E_\eta+K_{\eta z} \quad (8b)$$
$$M_s=D_m+E_s+K_{sz} \quad (8c)$$

For convenience of mathematical manipulation, the depth-averaged terms $\bar{u}$ and $\bar{c}$ can be represented by cross-sectionally averaged terms U and C and deviations U' and C', i.e.,

$$\bar{u}(s,\eta)=U+U'(s,\eta)=U+UF(s,\eta) \quad (9a)$$
$$\bar{c}(s,\eta)=C(s)+C'(s,\eta)=C(s)+C(s)G(s,\eta) \quad (9b)$$

where $F(s,\eta)$ and $G(s,\eta)$ are subject to the following constraints:

$$\int_0^B Fh\,d\eta=0$$
$$\int_0^B Gh\,d\eta=0 \quad (10)$$

in which h = local flow depth, and B = channel width.

Substituting Eq. (9) into Eq. (8a) and noting $\partial C/\partial \eta=0$ yields

$$\frac{\partial[C(1+G)]}{\partial t}+U\frac{\partial[C(1+G)(1+F)]}{\partial s}+C\frac{\partial(1+G)\bar{v}}{\partial \eta}=\frac{1}{h}\frac{\partial}{\partial s}\left(hM_s\frac{\partial C(1+G)}{\partial s}\right)+\frac{C}{h}\frac{\partial}{\partial \eta}\left(hM_\eta\frac{\partial G}{\partial \eta}\right) \quad (11)$$

In a coordinate system moving with the mean flow velocity U along the s direction, $x=s-Ut$, $y=\eta$, Eq. (11) is

$$\frac{\partial(1+G)C}{\partial t}+UF\frac{\partial C(1+G)}{\partial x}+UC(1+G)\frac{\partial F}{\partial x}+C\frac{\partial(1+G)\bar{v}}{\partial y}=\frac{1}{h}\frac{\partial}{\partial x}\left(hM_x\frac{\partial C(1+G)}{\partial x}\right)+\frac{C}{h}\frac{\partial}{\partial y}\left(hM_y\frac{\partial G}{\partial y}\right) \quad (12)$$

where $\bar{v}$ = average lateral velocity of the secondary current or helix flow and thus $\bar{v}\approx 0$. The lateral deviation of the concentration CG is much smaller than the mean concentration C in a cross section. The decay of concentration $\partial C/\partial t$ is assumed to be much smaller than the longitudinal concentration gradient term. Thus, the first and the last terms on the left hand side of Eq. (12) can be neglected. Furthermore, on the right hand side the depth and concentration gradients are much greater in the lateral than in the longitudinal direction (Fischer 1967), and therefore the first term can be eliminated. All this leads to

$$UF\frac{\partial C}{\partial x}+UC\frac{\partial F}{\partial x}=\frac{C}{h}\frac{\partial}{\partial y}\left(hM_y\frac{\partial G}{\partial y}\right) \quad (13a)$$

Fischer's approach does not contain the second term, which is attributed to the nonuniform velocity distribution of the flow in meandering streams. Eq. (13a) can be also written in the form

$$\frac{\partial(UFC)}{\partial x}=\frac{C}{h}\frac{\partial}{\partial y}\left(hM_y\frac{\partial G}{\partial y}\right) \quad (13b)$$

Eq. (13b) indicates that a scalar maintains a balance between the longitudinal advective mass transport caused by the shear velocity and the transverse mixing mass transport. Multiplying both sides of Eq. (13a) with h and integrating along y give an expression for $hM_y\partial G/\partial y$. Dividing by hM_y and integrating once more gives

$$C(x)G(y)=U\frac{\partial C}{\partial x}\int_0^y\frac{1}{hM_y}\int_0^y hF\,dy\,dy + UC\int_0^y\frac{1}{hM_y}\int_0^y h\frac{\partial F}{\partial x}dy\,dy + C(x)G(0) \tag{14}$$

The rate of longitudinal mass transport, relative to the moving coordinate axis, is given by

$$\frac{\partial M_{\text{ass}}}{\partial t}=\int_0^B hU'(y)C'(x,y)dy = \int_0^B h(UF)(CG)dy = UC\int_0^B hFG\,dy \tag{15}$$

where the integration is performed over the full width. It should be noted that the integration over width B makes sense only when the lateral mixing process of constituents has been completed across the whole flow width.

Substituting Eq. (14) into Eq. (15) and recalling the first equality of Eq. (10) result in

$$\frac{\partial M_{\text{ass}}}{\partial t}=U^2\int_0^B hF\left(\frac{\partial C}{\partial x}\int_0^y\frac{1}{hM_y}\int_0^y hF\,dy\,dy + C\int_0^y\frac{1}{hM_y}\int_0^y h\frac{\partial F}{\partial x}dy\,dy\right)dy \tag{16}$$

The rate of mass transport in the longitudinal direction can also be defined in terms of a longitudinal mixing coefficient, with an analogy to the molecular diffusion coefficient (Fischer et al. 1979) as

$$\frac{\partial M_{\text{ass}}}{\partial t}=-AK_x\frac{\partial C}{\partial x} \tag{17}$$

where $A=BH=$cross-sectional area of the river channel; H =mean flow depth; and $K_x=$longitudinal dispersion coefficient related to the integration over the whole channel cross-section and is thus the most important mixing parameter. Equating Eqs. (16) and (17) yields

$$K_x=-\frac{U^2}{A}\int_0^B hF\left(\int_0^y\frac{1}{hM_y}\int_0^y hF\,dy\,dy + \frac{C}{\partial C/\partial x}\int_0^y\frac{1}{hM_y}\int_0^y h\frac{\partial F}{\partial x}dy\,dy\right)dy \tag{18}$$

where the last term is attributed to the nonuniformity of flow. Introducing dimensionless width coordinate ξ

$$\xi=\frac{y}{B} \tag{19a}$$

and dimensionless depth h_*

$$h_*=\frac{h(y)}{h_{\max}}=\frac{h(\xi)}{h_{\max}} \tag{19b}$$

where $h_{\max}=$maximum flow depth in a cross section.

The transverse mixing coefficient M_y can be expressed as (Deng et al. 2001)

$$M_y=M_*hu^* \tag{20a}$$

with the dimensionless transverse mixing coefficient M_* being

$$M_*=0.145+\frac{1}{3{,}520}\left(\frac{U}{U^*}\right)\left(\frac{B}{H}\right)^{1.38} \tag{20b}$$

where $h=$local flow depth; $u^*=$local shear velocity; and U^* =cross-sectional shear velocity. The local shear velocity and the maximum shear velocity in a cross section are expressed as

$$u^*=\gamma\sqrt{gSh}$$

and

$$u^*_{\max}=\gamma\sqrt{gSh_{\max}} \tag{21}$$

where $S=$channel slope; $g=$acceleration due to gravity; and γ =correction factor to get a correct cross-sectional shear velocity. Introducing the dimensionless depth h_*, it is seen that

$$u^*=u^*_{\max}\sqrt{h_*} \tag{22}$$

The mean shear velocity in a cross section is obtained by integrating the local shear velocity over the width

$$\overline{u^*}=\gamma\sqrt{gSh_{\max}}\int_0^1\sqrt{h_*}d\xi=u^*_{\max}\int_0^1\sqrt{h_*}d\xi \tag{23}$$

This mean value should correspond to the cross-sectional shear velocity

$$U^*=\sqrt{gRS} \tag{24}$$

where R is hydraulic radius. Comparing Eqs. (23) and (24) it is seen that

$$\gamma=\sqrt{\frac{R}{h_{\max}}}\left(\int_0^1\sqrt{h_*}d\xi\right)^{-1} \tag{25}$$

The ratio between the cross-sectional shear velocity and the maximum shear velocity is obvious from Eq. (23) and is

$$I_*=\frac{U^*}{u^*_{\max}}=\int_0^1\sqrt{h_*}d\xi \tag{26}$$

Also the cross-section average flow depth H can be related to the maximum depth and expressed in dimensionless form H_*:

$$H_*=\frac{H}{h_{\max}}=\int_0^1 h_*d\xi \tag{27}$$

Returning to the expression for M_y, Eq. (20*a*), replacing the local shear velocity with the maximum cross section shear velocity, gives

$$M_y=M_*h_{\max}u^*_{\max}h_*^{3/2} \tag{28}$$

Replacing variables y, h, and M_y in Eq. (18) with their dimensionless forms ξ, h_*, and M_* by means of Eqs. (19) and (28), one obtains

$$K_x=-\frac{U^2}{u^*_{\max}M_*}\frac{B^2}{H}\int_0^1 h_*F\left(\int_0^\xi zh_*^{-5/2}\int_0^\xi h_*F\,d\xi\,d\xi + \frac{C}{\partial C/\partial x}\int_0^\xi h_*^{-5/2}\int_0^\xi h_*\frac{\partial F}{\partial x}d\xi\,d\xi\right)d\xi \tag{29}$$

Expressing $u^*_{\max}$ in terms of I_* and U_* on the basis of Eq. (26) and inserting it into Eq. (29) yields

$$\frac{K_x}{U^*H}=-\left(\frac{I_*I_0}{M_*}\right)\left(\frac{U}{U^*}\right)^2\left(\frac{B}{H}\right)^2 \tag{30a}$$

with

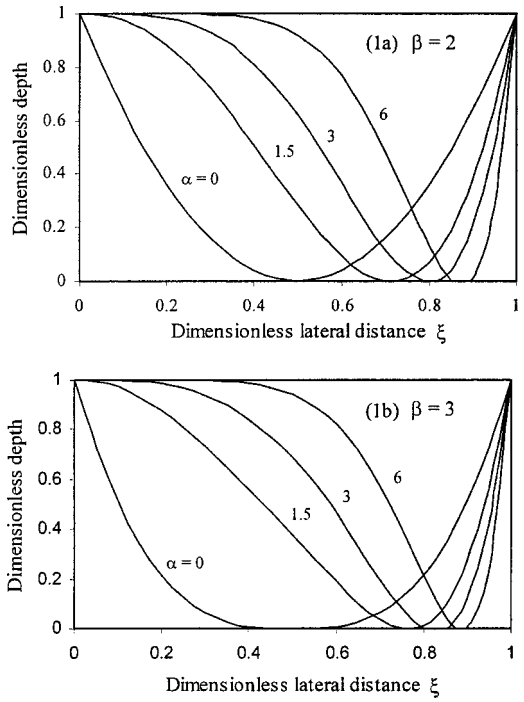

Fig. 1. Channel shape change with α and β

$$I_0 = \int_0^1 h_* F \left(\int_0^\xi h_*^{-5/2} \int_0^\xi h_* F d\xi \, d\xi + \frac{C}{\partial C/\partial x} \int_0^\xi h_*^{-5/2} \int_0^\xi h_* \frac{\partial F}{\partial x} d\xi \, d\xi \right) d\xi \tag{30b}$$

The ξ coordinate is shown in Fig. 1 reflecting the variation of the dimensionless local flow depth h_* with the channel shape parameter β and skewness parameter α and the location ξ. Let $I = I_* I_0$, then Eq. (30*a*) can be rewritten as

$$\frac{K_x}{U^* H} = -\left(\frac{I}{M_*}\right)\left(\frac{U}{U^*}\right)^2 \left(\frac{B}{H}\right)^2 \tag{30c}$$

Eq. (30) is the basic equation of the longitudinal dispersion coefficient K_x. As compared to Fischer's expression of the longitudinal dispersion coefficient, Eq. (30) is characterized by two distinct features: (1) The transverse mixing coefficient in Eq. (30) contains both the lateral turbulent diffusion coefficient, included in Fischer's triple integration, and the lateral dispersion coefficient, produced by the depth integration and discarded in the analysis of Fischer and Taylor (Fischer et al. 1979). (2) The second term in Eq. (30*b*) reflects the characteristics of flow in meandering rivers. The contribution from this term becomes significant when secondary currents are strong. The variation of the dimensionless velocity deviation $\partial F/\partial x$ attains the maximum at river bends and becomes zero or negligible in straight reaches. The expression of I_0 reduces to Fischer's triple integration for straight rivers without secondary currents. In Eq. (30) the channel width B, the mean flow depth H, the mean velocity U, and the shear velocity U^* are readily available bulk hydraulic variables for natural streams, but the other dimensionless parameters need to be determined.

Parameter Determination

Concentration Related Term $C/(\partial C/\partial x)$

For a one-dimensional advection–diffusion equation, a simple steady-state analytical solution can be obtained (Martin and McCutcheon 1999) as

$$C = C_0 \exp\left(-\frac{Ux}{K_{x0}}\right) \tag{31a}$$

Eq. (31*a*) leads to

$$\frac{C}{\partial C/\partial x} = -\frac{K_{x0}}{U} \tag{31b}$$

Eq. (31*b*) indicates that the ratio of the concentration C and its derivative with respect to the longitudinal distance x is a constant if K_{x0} and U are regarded as constant along the stream. K_x in Eq. (30) is different from K_{x0} in Eq. (31) which can be understood as the longitudinal dispersion coefficient in the straight stream.

Velocity Deviation Parameter F

It is seen from Eq. (9*a*) that the dimensionless parameter F represents the deviation of the depth-averaged velocity $u(s,\eta)$ (the double overbar is dropped hereafter) from the cross-sectional mean U. It is assumed that the local velocity $u(s,\eta)$ can be calculated from one of the uniform-flow formulas of Manning, Chezy, Darcy-Weisbach, among others (Chow 1959; Chang 1988) by the incorporation of a correction factor ϕ'. The local velocity is then

$$u = \phi' a \sqrt{S} h^b \tag{32}$$

where a = Chezy coefficient and $b = 1/2$ for the Chezy formula; $a = 1/n$ (n = Manning roughness coefficient) and $b = 2/3$ for Manning formula; $a = (8g/f)^{0.5}$ (f = dimensionless friction factor) and $b = 1/2$ for Darcy–Weisbach formula; ϕ' is actually a factor localizing the cross-sectional formula

$$U = a \sqrt{S} R^b \tag{33}$$

to individual verticals in the cross section. Then the velocity deviation parameter F can be expressed in terms of the local flow depth h and the hydraulic radius R or the cross-sectional averaged depth H that is used more frequently than R as

$$F = \frac{u}{U} - 1 = \frac{\phi' a \sqrt{S} h^b}{a \sqrt{S} R^b} - 1 = \phi' \left(\frac{h}{R}\right)^b - 1 = \phi \left(\frac{h}{H}\right)^b - 1 = \phi \left(\frac{h_*}{H_*}\right)^b - 1 \qquad \left[\phi = \phi' \left(\frac{H}{R}\right)^b\right] \tag{34}$$

It is apparent that the correction factor ϕ accounts for the influences of the localization and the replacement of R by H. The introduction of ϕ is to assure that the integrated local velocity corresponds to the mean velocity. Therefore, ϕ is subject to the constraint of Eq. (10), i.e.,

$$\int_0^1 \left[\phi \left(\frac{h_*}{H_*}\right)^b - 1\right] h_* \, d\xi = 0 \tag{35}$$

The value of ϕ can be determined by a trial and error method when the numerical integral value of Eq. (35) is very close to zero

and no longer changes markedly with a new value of ϕ. The correction factor ϕ is absolutely necessary to obtain an accurate and stable numerical value of I_0. With ϕ known, the dimensionless parameter F the deviation of the dimensionless velocity from the cross-sectional mean, can be determined from Eq. (34), and thereby the triple integration I can be evaluated from Eqs. (30*b*) and (26) if the dimensionless flow depth h_* is known. Parameter F may also be determined if field measurements of the transverse distribution of u/U are available (Appendix II). It appears that all the unknowns in Eq. (30) are related to h_*, therefore, a determination of the dimensionless flow depth h_* is essential to the practical application of Eq. (30).

Local Flow Depth h_*

Based on the at-a-station hydraulic geometry relationship of stable alluvial rivers a local flow depth equation for straight streams in a channel center symmetrical coordinate system was derived as follows (Deng et al. 2001):

$$h_* = 1 - \xi^{\beta}, \quad [\beta = \ln(B/H)] \tag{36a}$$

where β = channel shape parameter, the dimensionless lateral coordinate or distance ξ was measured from channel center (coordinate origin) due to the symmetry of the cross-sectional shape around the channel center for straight streams. It should be noted that the absolute value of ξ should be used for $\xi < 0$. If the origin of the coordinate system is set at one bank of the stream, as shown in Fig. 1, then Eq. (36*a*) assumes the following form:

$$h_* = 1 - (|2\xi - 1|)^{\beta} \tag{36b}$$

The cross-sectional channel shape of straight streams is symmetrical at least in theory or in a statistical sense, as shown in Fig. 8(b). However, meandering streams are characterized by the asymmetrical cross-sectional channel shape with a series of riffle-pool structures. The position of the maximum channel or flow depth at a cross section varies alternatively from one bank to another and reaches the channel center in straight reaches between the two consecutive pools along the stream. It means that: (1) the local flow depth in meandering streams varies both laterally and longitudinally even for steady flow; and (2) Eq. (36*b*) should be a special case of the cross-sectional shape equation of meandering streams. To that end, a new channel shape equation is assumed for meandering streams as follows:

$$\frac{h}{h_{\max}} = h_* = \frac{\xi^{\alpha}}{P}(1 - |2\xi - 1|^{\beta}) \quad 0 \leq \xi \leq 1 \tag{37a}$$

$$\alpha = 3\left[1 - \sin\left(\frac{\pi x}{2L}\right)\right](\sigma - 1)^{\delta} \quad \delta = 0.5$$

$$\text{for } \sigma > 2 \text{ and } \delta = 1 \text{ for } \sigma < 2 \tag{37b}$$

where the denominator P is introduced to ensure a unity for the maximum dimensionless depth h_* and thus P is equal to the maximum value of the numerator. α is a parameter used to reflect the skewness of the cross-sectional channel shape and is determined based on the fact that the values of the dispersion coefficients obtained by Deng et al. (2001) correspond to those of the streams with sinuosity $\sigma = 1.6$ and $\beta = 3$ as alluvial streams tend to form a stable channel pattern with $\sigma \approx 1.6$ and $\beta = 3$ in a statistical sense (Deng and Singh 1999). σ is the channel sinuosity, defined as the ratio of the valley slope to the channel slope, or the ratio of the channel length to the valley length (Chang 1988), i.e., $\sigma = 4L/L_m$. L = one fourth of the arc length or the distance from apex to entrance or to exit along the meander path; L_m = meander wavelength; x = distance measured along the meander path; and $x = 0$ at the apex and $x = L$ at the entrance or exit of a bend, as shown in Fig. 2. It should be pointed out that Eq. (37*b*) is an empirical result based on the sine-generated channel curve (Chang 1988; Przedwojski et al. 1995) and fitting of Eq. (37*a*) to some measured cross-sectional channel shapes of natural streams.

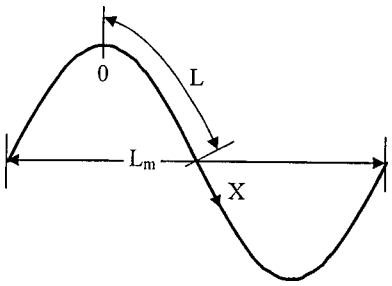

Fig. 2. Natural coordinate system

Eq. (37*a*) reduces to Eq. (36*b*) when $\alpha = 0$ ($\sigma = 1$ or $x = L$). Parameter P can be determined by differentiating the channel shape equation with respect to lateral distance ξ. For the coordinate system shown in Fig. 1, the coordinate origin is located on the convex bank, and $h_{\max}$ should occur in the range of $0.5 < \xi \leq 1$. Thus, Eq. (37*a*) is employed to determine the location of $h_{\max}$. Let

$$p = \xi^{\alpha}[1 - (2\xi - 1)^{\beta}] \tag{38}$$

It is apparent that $p = 0$ when $\xi = 1$, and p reaches its maximum P when $0.5 < \xi = \xi_c \leq 1$ for $\alpha \neq 0$. ξ_c is the lateral coordinate of $h_{\max}$. Differentiating Eq. (38) with respect to ξ and equating it to zero yields

$$\alpha - \alpha(2\xi - 1)^{\beta} - 2\beta\xi(2\xi - 1)^{\beta - 1} = 0 \tag{39}$$

For a specific cross section along the river channel, α and β are known, ξ_c can be solved from Eq. (39). Then, substituting ξ_c into Eq. (38) results in

$$P = \xi_c^{\alpha}[1 - (2\xi_c - 1)^{\beta}] \tag{40}$$

An approximate but simple method of determining P and ξ_c is to take the maximum value of P corresponding to $\xi = 0.525$, 0.555, 0.575, ..., and 1. $\xi_c = 0.5$ for $\alpha = 0$ or straight river reaches. The variation of h_* with α and β is plotted in Fig. 1, where the vertical coordinate actually denotes $(1 - h_*)$. With h_* defined, the dimensionless parameters H_*, I_*, and I can be determined as

$$H_* = \int_0^1 h_* d\xi = \frac{1}{P}\left\{\int_0^{0.5} \xi^{\alpha}[1 - (1 - 2\xi)^{\beta}]d\xi + \int_{0.5}^1 \xi^{\alpha}[1 - (2\xi - 1)^{\beta}]d\xi\right\} \tag{41}$$

$$I_* = \int_0^1 \sqrt{h_*} d\xi = \frac{1}{\sqrt{P}}\left\{\int_0^{0.5} \sqrt{\xi^{\alpha}[1 - (1 - 2\xi)^{\beta}]}d\xi + \int_{0.5}^1 \sqrt{\xi^{\alpha}[1 - (2\xi - 1)^{\beta}]}d\xi\right\} \tag{42}$$

Eqs. (41)–(42) can be solved by numerical integration. Depending on Eqs. (34) and (58) of the velocity deviation parameter F, parameter I_0 can be determined from two approaches: In the first approach, Eq. (34) is employed to determine F and $\partial F/\partial x$

Table 1. Simplified Expressions of Triple Integration I

β	B/H	Regression equation	R^2
2.3	10	$I=0.0061\sigma^3-0.0259\sigma^2+0.0422\sigma-0.0224$	0.9969
3.0	20	$I=0.0077\sigma^3-0.0379\sigma^2+0.0686\sigma-0.0387$	0.9983
4.0	54.6	$I=0.0094\sigma^3-0.0502\sigma^2+0.0954\sigma-0.0553$	0.9972
5.0	148.4	$I=0.0105\sigma^3-0.058\sigma^2+0.112\sigma-0.0651$	0.9972

$$\frac{\partial F}{\partial x}=\frac{\phi}{H_*^b}\frac{\partial h_*^b}{\partial x}+\phi h_*^b\frac{\partial}{\partial x}\left(\frac{1}{H_*^b}\right) \tag{43}$$

It is seen from Eq. (41) that the variability of H_* is significantly reduced due to the lateral integration as compared to h_*. It signifies that the second term on the right hand side of Eq. (43) is significantly smaller than the first term. The second term is assumed to be equal to the first term multiplied by a coefficient ψ. Then, $\partial F/\partial x$ can be simplified as

$$\frac{\partial F}{\partial x}=\phi(1+\psi)\frac{bh_*^{b-1}}{H_*^b}\frac{\xi^\alpha[1-(|1-2\xi|)^\beta]}{P}(\ln\xi)\times\left[-3(\sigma-1)^\sigma\frac{\pi}{2L}\cos\left(\frac{\pi x}{2L}\right)\right] \tag{44}$$

The arc length $4L$ of meandering channels varies in a wide range around $2\pi B$ (Chang 1988; Przedwojski et al. 1995). It is thus assumed that $L=(1+\psi)\pi B/2$. Then,

$$\frac{\partial F}{\partial x}=-\frac{3b\phi}{H_*^b}\frac{(\sigma-1)^\delta}{B}\cos\left(\frac{\pi x}{2L}\right)h_*^b\ln(\xi) \tag{45}$$

Substitution of Eqs. (31), (34), and (45) into Eq. (30*b*) leads to

$$I_0=\int_0^1 h_*\left(\phi\frac{h_*^b}{H_*^b}-1\right)\left[\int_0^\xi h_*^{-5/2}\int_0^\xi\left(\phi\frac{h_*^b}{H_*^b}-1\right)h_*d\xi\,d\xi+\left(\frac{K_{x0}}{UB}\right)\left(\frac{3b\phi}{H_*^b}\right)(\sigma-1)^\delta\times\cos\left(\frac{\pi x}{2L}\right)\int_0^\xi h_*^{-5/2}\int_0^\xi h_*^{b+1}(\ln\xi)d\xi d\xi\right]d\xi \tag{46}$$

where cos( ) should take its absolute value when it is less than zero. It is interesting to find that K_{x0}/UB can be taken as a constant of 3, i.e., $K_{x0}\approx 3UB$, as listed in Table 2. Actually, the accuracy of $K_{x0}\approx 3UB$ is comparable with that of the most accurate empirical formula without the consideration of the influence of channel meandering. If the Manning formula of uniform flow is used, then the exponent $b=2/3$, and Eq. (46) can be recast into

$$I_0=\int_0^1 h_*\left(\phi\frac{h_*^{2/3}}{H_*^{2/3}}-1\right)\left[\int_0^\xi h_*^{-5/2}\int_0^\xi\left(\phi\frac{h_*^{2/3}}{H_*^{2/3}}-1\right)h_*d\xi\,d\xi+\left(\frac{6\phi}{H_*^{2/3}}\right)(\sigma-1)^\delta\cos\left(\frac{\pi x}{2L}\right)\int_0^\xi h_*^{-5/2}\int_0^\xi h_*^{5/3}(\ln\xi)d\xi\,d\xi\right]d\xi \tag{47}$$

In the second (Chezy) approach to determine I_0, Eq. (58) is employed to determine F and $\partial F/\partial x$ in the same way as the first approach, then one gets

$$\frac{\partial F}{\partial x}=(1+\psi)\frac{f_u h_*^{-1/2}}{2H_*^{1/2}}\frac{\xi^\alpha[1-(|1-2\xi|)^\beta]}{P}(\ln\xi)\times\left[-3(\sigma-1)^\delta\frac{\pi}{2L}\cos\left(\frac{\pi x}{2L}\right)\right]=-\frac{3}{2}\frac{(\sigma-1)^\delta}{BH_*^{0.5}}f_u\cos\left(\frac{\pi x}{2L}\right)h_*^{1/2}\ln(\xi) \tag{48}$$

Substitution of Eqs. (31), (58), and (48) into Eq. (30*b*) results in

$$I_0=\int_0^1 h_*\left[\theta f_u\left(\frac{h_*}{H_*}\right)^{1/2}-1\right]\times\left(\int_0^\xi h_*^{-5/2}\int_0^\xi\left[\theta f_u\left(\frac{h_*}{H_*}\right)^{1/2}-1\right]h_*d\xi\,d\xi+\frac{9}{2}\frac{(\sigma-1)^\delta}{H_*^{0.5}}\cos\left(\frac{\pi x}{2L}\right)\int_0^\xi h_*^{-5/2}\times\int_0^\xi f_u h_*^{3/2}(\ln\xi)d\xi\,d\xi\right)d\xi \tag{49}$$

Eq. (49) is employed mainly to check the validity of the application of uniform flow equations to local flow. The correction factor θ in Eq. (49) has the same function as ϕ, but θ ranges from around 0.48 to 0.60. From Eq. (47) I_0 can be calculated for each cross section in a stream reach and then the results are compared with that from Eq. (49) for sinuosity $\sigma>1.6$. Eqs. (47) and (49) indicate that the triple integration I_0 varies with both the channel sinuosity and the width–depth ratio.

Simplification of Triple Integration

In order to use Eq. (30) easily in practice, a set of regression equations is provided in Table 1 for the most possible range of channel shape parameter based on the results of the numerical integration, conducted for $\sigma=1$, 1.1, 1.2, 1.4, 1.6, 1.8, 2, 2.2, 2.4, 2.6, 2.8, and 3, respectively, as indicated in Figs. 3(a–c) and Fig. 4.

The numerical integration is conducted for $\sigma=1-3$ and $\beta=2.3-5$ as the channel sinuosity of alluvial streams ranges from 1 to 3 in general (Schumm 1963). Most meandering streams possess the width to depth ratio ranging from 10 to 150. Streams with $B/H>150$ generally have a straight channel pattern (Deng and Singh 1999). The width to depth ratio of some straight canals may be less than 10. Therefore, a regression equation of I is given for straight streams as shown in Fig. 5, where the I values are plotted against the channel width to depth ratio as in the case of $\sigma=1$ the expression (37*a*) of h_* contains only one parameter $\beta=\ln(B/H)$. Table 1 just lists four cases of the width to depth ratio. For other cases the I value can be linearly interpolated from the neighboring values computed from the corresponding regression

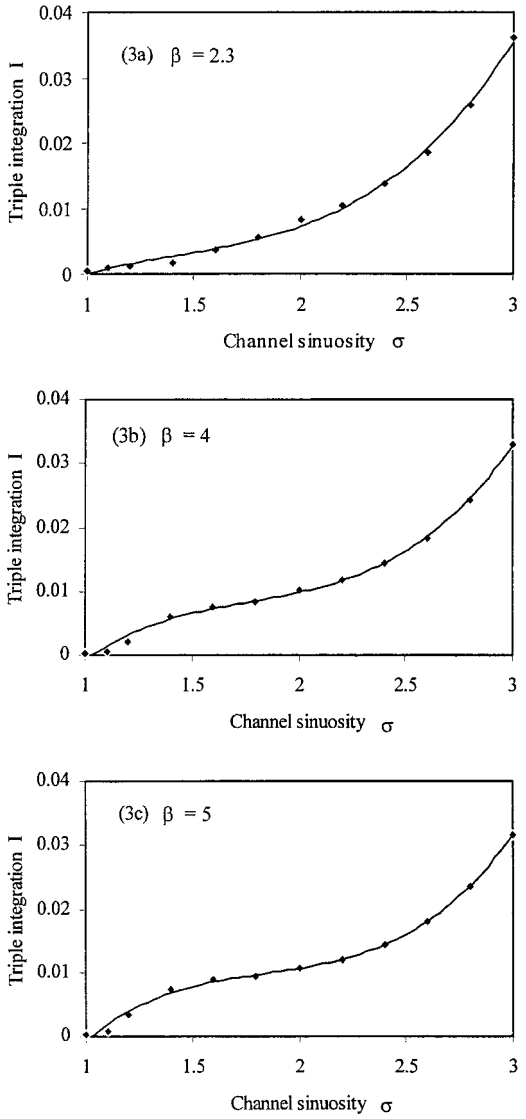

Fig. 3. Variation of triple integration I with σ and β

equations. The results of numerical integration illustrate that both Eqs. (47) (Manning approach) and (49) (Chezy approach) lead to comparable I values for $\beta > 1.6$, as Eq. (59*a*) is applicable to $\beta > 1.6$, due to the introduction of the velocity correction factor θ. The results of Eq. (49) with f_u calculated from Eq. (59*b*) approach that of Eq. (47) corresponding to $\sigma = 1.08-1.11$ for different β values. Such a result is easily understood as natural streams scarcely follow a straight alignment with $\sigma = 1.0$. It means that the uniform flow equation with the revisions made in the paper is applicable to local flow. Consequently, all the regression equations employ the I_0 values from Eq. (47). It should be pointed out that all the I values used in a regression analysis of the equations in Table 1 are the average of the I values at cross sections $x=0$ and L, i.e., $I=(I_{x=0}+I_{x=L})/1.57$, where 1.57 instead of 2 is used due to the sine-generated channel curve of natural streams. The influence of channel meandering on the value of the triple integration defined in Eq. (30) is demonstrated in Fig. 4, where the one-term curve represents the I values calculated from the first term of Eq. (30*b*) in combination with Eq. (26), and the two-term curve refers to the result incorporating the contributions of all the two terms in Eq. (30*b*). Except for the case of σ approaching unity that is the implicit assumption of most existing empirical formulas of the longitudinal dispersion coefficient, the influence of the second term on the I value is significant. In fact, Fig. 4 indicates that the second term—the change of the nonuniformity of flow along the channel—plays a more important role than the first term in the longitudinal dispersion process of the moderately meandering streams with $\sigma = 1.25-1.85$ that is the channel sinuosity range of most natural streams (Deng and Singh 1999). It means that for the most frequently occurring natural streams, the second term is the controlling mechanism underlying the longitudinal dispersion. However, all the existing empirical methods fail to comprise this term. As a result, the predicted longitudinal dispersion coefficients deviate from observed ones by orders of magnitude. Owing to the incorporation of the second term, Eq. (30) should significantly improve the prediction of the longitudinal dispersion in natural streams in principle. To that end, a vast number of field observations are employed to test the performance of Eq. (30).

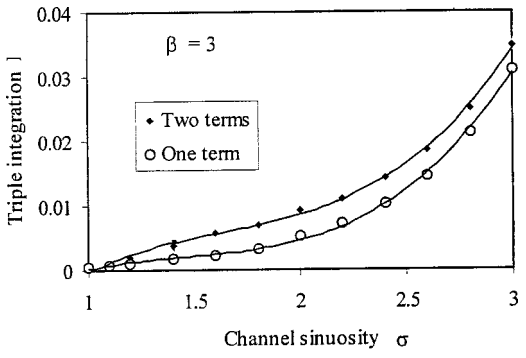

Fig. 4. Influence of channel meandering on triple integration

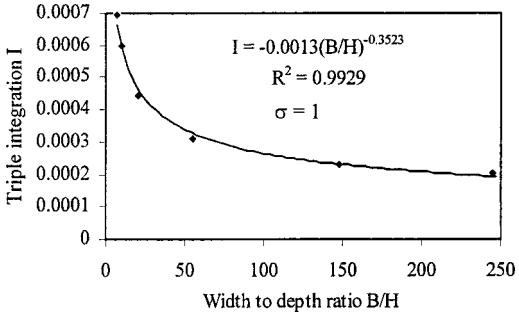

Fig. 5. Variation of triple integration I with B/H

Verification of Proposed Method

70 sets of field data measured on 30 streams in the United States were used to test the accuracy and feasibility of the method developed for prediction of the longitudinal dispersion coefficient in natural streams, including straight and meandering ones. Among the 70 data sets, 59 were collected from Seo and Cheong (1998), and the remaining 11 from Godfrey and Frederick (1970); Yotsukura et al. (1970); and McQuivey and Keefer (1974), the data of channel sinuosity were calculated from 1:25,000 scale topographic maps based on the specific stream reaches of dye tests described by Nordin and Sabol (1974) and in the above-mentioned reports. In Table 2, the third column is the channel width to depth ratio; the fourth column gives the ratio of flow

Table 2. Comparison of Measured and Predicted Longitudinal Dispersion Coefficients

Number	River reach	B/H	U/U^*	M_*	DISPERSION COEFFICIENT K_g (m^2/s)					
					Measured value	Predicted by Deng	Predicted by Fischer	$3UB$	I ratio	σ
1	Antietam Creek, Md.	42.7	7.36	0.517	17.50	16.8	18.6	16.1	14.9	1.40
2		24.6	6.02	0.287	101.50	85.0	23.1	42.6	27.6	2.25
3		18.0	5.06	0.223	20.90	23.8	5.1	15.3	24.2	2.25
4		43.8	8.98	0.615	25.90	30.7	56.4	39.1	10.7	1.26
5	Monocacy River, Md.	88.5	5.00	0.836	37.80	31.0	61.7	38.0	17.3	1.28
6		130.9	3.48	0.970	41.40	35.4	74.5	44.6	21.7	1.28
7		78.8	14.09	1.803	29.60	87.5	387.7	95.2	16.0	1.28
8		84.8	5.51	0.864	119.80	132.3	160.7	93.6	28.8	1.61
9		98.9	5.75	1.070	66.50	39.9	58.3	28.0	31.2	1.61
10	Conococheague Creek, Md.	61.2	3.59	0.443	40.80	59.4	23.5	29.1	40.4	2.25
11		121.2	1.85	0.540	29.30	39.3	18.4	22.4	52.9	2.25
12		38.0	7.78	0.480	53.30	67.5	88.1	81.2	11.2	1.31
13	Chattahoochee River, Ga.	38.8	5.36	0.382	88.90	109.7	127.9	167.8	10.1	1.27
14		37.7	5.53	0.380	166.90	163.8	109.5	143.4	17.3	1.57
15	Salt Creek, Neb.	64.0	6.31	0.703	52.20	24.7	34.1	23.0	18.6	1.38
16	Difficult Run, Va.	46.7	4.03	0.376	1.90	2.1	7.5	10.9	3.5	1.09
17	Bear Creek, Colo.	16.1	2.33	0.176	2.90	3.0	7.3	53.1	1.6	1.08
18	Little Piney Creek, Mo.	72.0	7.35	0.910	7.10	7.5	36.0	18.5	7.2	1.13
19	Bayou Anacoco, La.	39.0	13.33	0.738	5.80	20.1	32.0	16.8	14.2	1.41
20	Comite River, La.	68.3	9.23	1.036	69.00	16.5	39.2	16.9	16.4	1.31
21	Bayou Bartholomew, La.	23.8	6.45	0.291	54.70	54.2	11.3	20.0	36.1	2.46
22	Amite River, La.	41.0	20.00	1.102	501.40	257.6	104.0	34.6	85.4	2.93
23	Tickfaw River, La.	25.3	3.38	0.228	10.30	10.3	3.8	12.1	16.4	1.75
24	Tangipahoa River, La.	38.8	6.67	0.440	45.10	60.6	42.8	45.2	19.1	1.46
25		74.7	17.00	2.002	44.00	41.8	141.8	30.5	22.8	1.46
26	Red River, La.	156.5	19.06	5.929	143.80	206.8	5077.5	464.1	17.9	1.20
27		40.8	4.83	0.374	130.50	133.9	101.6	140.5	15.4	1.44
28		41.6	7.89	0.530	227.60	230.7	248.0	205.7	15.5	1.44
29		89.2	13.05	1.967	177.70	172.6	933.6	218.7	15.0	1.24
30	Sabine River, La.	70.6	10.74	1.230	131.30	129.0	563.0	202.6	10.7	1.19
31		69.1	19.63	2.072	308.90	307.1	2535.7	509.8	9.4	1.17
32	Sabine River, Tex.	28.3	3.51	0.246	12.80	12.7	2.0	5.5	42.4	2.53
33		23.9	7.67	0.319	14.70	14.7	5.6	8.4	21.5	2.05
34		22.9	10.28	0.366	24.20	24.0	19.9	23.0	11.2	1.47
35	Mississippi River, La.	35.7	13.65	0.683	237.20	181.9	2134.2	1194.8	14.1	1.44
36	Mississippi River, Mo.	108.0	15.22	2.910	457.70	382.5	10123	1680.2	24.4	1.38
37		60.4	15.56	1.414	374.10	583.9	8389.7	2434.3	18.0	1.38
38	Wind/Bighorn River, Wyo.	32.3	6.97	0.384	184.60	151.6	108.3	131.3	15.5	1.56
39		35.8	11.37	0.596	464.60	609.1	666.1	445.5	16.3	1.56
40	Copper Creek, Va.	34.0	2.50	0.237	16.84	20.5	3.1	10.0	45.8	2.54
41	Clinch River, Va.	41.8	3.04	0.294	14.76	15.4	14.2	30.5	10.0	1.25
42	Copper Creek, Va.	48.1	1.29	0.222	20.71	13.2	1.9	8.2	51.8	2.54
43	Powell River, Tenn.	42.3	2.41	0.265	15.50	20.9	5.4	14.3	32.7	2.20
44	Clinch River, Va.	47.0	5.07	0.437	10.70	11.1	26.3	30.1	6.1	1.14
45	Copper River, Va.	23.3	4.85	0.252	20.82	13.3	12.0	28.8	7.2	1.26
46	Clinch River, Va.	23.6	7.21	0.306	40.49	41.3	81.4	130.3	4.0	1.14
47		22.1	6.17	0.270	36.93	29.8	52.7	105.4	3.9	1.14
48	Copper Creek, Va.	35.7	3.00	0.263	24.62	28.1	4.7	12.1	46.6	2.54
49	Missouri River, Iowa	62.2	22.09	2.021	1486.4	1355.4	4852.0	962.9	20.1	1.44
50	Bayou Anacoco, La.	27.6	5.07	0.285	32.52	19.8	13.6	26.4	11.4	1.41
51		40.2	5.97	0.422	39.48	42.7	38.6	43.9	14.5	1.41
52	Nooksack River, Wash.	84.2	2.50	0.467	34.84	93.8	99.3	128.7	17.8	1.30
53	Wind/Bighorn River, Wyo.	54.0	7.39	0.662	41.81	88.4	229.9	156.9	8.8	1.18
54		31.8	9.22	0.455	162.58	161.8	342.5	318.9	6.1	1.18
55	John Day River, Ore.	43.1	7.21	0.514	13.94	14.9	86.3	75.7	2.8	1.08
56		13.8	4.56	0.194	65.03	60.2	19.4	84.0	12.8	1.89

Table 2. (*Continued*)

Number	River reach	B/H	U/U^*	M_*	DISPERSION COEFFICIENT K_g (m^2/s)					
						Predicted by				
					Measured value	Deng	Fischer	$3UB$	I ratio	σ
1										
57	Yadkin River, N.C.	29.8	4.26	0.276	111.48	147.8	42.1	90.4	27.1	2.17
58		18.7	5.94	0.241	260.13	257.2	66.3	163.3	22.1	2.17
59	Coachella Canal, Calif.	15.6	16.10	0.348	5.92	5.8	45.1	48.9	1	1.00
60	Nooksack, Wash.	29.4	2.26	0.213	153.0	118.0	75.4	309.6	9.3	1.30
61	Susquehanna, Pa.	150.4	6.00	1.867	92.9	97.5	785.7	237.5	11.5	1.13
62	Bayou Anacoco, La.	47.6	6.44	0.523	13.9	18.5	19.6	17.4	16.4	1.41
63	Missouri River, Iowa	78.5	13.48	1.724	465.0	541.0	1897.5	488.6	19.4	1.35
64		56.5	15.24	1.277	837.0	889.3	2434.9	771.8	16.3	1.35
65	Missouri River, Iowa	63.3	19.62	1.853	892.0	1057.2	4119.6	904.2	17.4	1.35
66	Chicago Ship Canal	6.0	14.14	0.193	3	4.0	12.4	39.5	1	1.00
67	Elkhorn River, Neb.	108.7	9.35	1.860	9.3	11.4	157.8	42.3	5.9	1.09
68	Elkhorn River, Neb.	121.2	9.91	2.258	20.9	19.3	311.5	70.7	6.4	1.09
69	Comite River, La.	48.1	7.01	0.562	7	10.3	14.4	11.6	13.3	1.31
70	Comite River, La.	38.5	6.60	0.434	13.9	14.0	16.3	17.5	11.4	1.31

velocity and shear velocity; the sixth column lists the values of the observed longitudinal dispersion coefficient; and the fifth column is the dimensionless transverse mixing coefficient M_* calculated from Eq. (20*b*). As there are no field data of M_* for the river reaches listed in Table 2, it is thus difficult to quantitatively determine the accuracy of Eq. (20). However, a qualitative comparison may enhance the confidence in application of Eq. (20). Lau and Krishnappan (1981) compiled 11 sets of field data for transverse dispersion coefficient. Except the highest value of $M_*=3.30$ for the Missouri River, the M_* values of all other rivers range from 0.22 to 1.0. Fischer et al. (1979) suggested $M_*=0.6\pm 50\%$ for moderately meandering streams. It is seen from Table 2 that the values of $0.18<M_*<0.9$ account for 70% of 70 data sets, although M_* ranges from 0.18 to 2.91 except for the extreme one of 5.93. Therefore, the calculated values of M_* are consistent at least qualitatively with the measured values. Using Eq. (30*c*) and the regression equations in Table 1 in combination with the interpolating method, the predicted dispersion coefficients were obtained and listed in the seventh column of Table 2. The results illustrate that the predicted dispersion coefficients by the new method are reasonably accurate as compared to the measured ones for $B<200$ m. Among the 70 sets of predicted and measured dispersion coefficients, 60 or 85.7% predictions fall within the range of $0.5<K_P(\text{predicted})/K_M(\text{measured})<2$. A step by step procedure for using the numerical integration and the regression equations to calculate the longitudinal dispersion coefficients is discussed in Appendix III.

It is found that the method overestimates K_x systematically when $B>200$ m. The predicted dispersion coefficients of data set No. 26 (Red River), No. 35–37 (Mississippi River) are 305.98, 1475.49, 1930.25, and 2982.81 m^2/s, respectively. The greater the channel width B, the higher the predicted K_x is than observations. Such an overestimation is attributed to the inconsistency of the mixing conditions required by the equation derived in this paper with the real dye test conditions. In theory, this method is applicable to the fully mixing stream reaches in the whole flow width. However, some dye tests were conducted on the partly mixing river reaches (McQuivey and Keefer 1976). It means that the actual mixing width is less than the channel width listed in Table 2, causing the overestimation. If an effective mixing width of 200 m is taken for the Red River and Mississippi River, 64 or 91.4% of the predictions fall within the range of $0.5<K_P/K_M<2$. It should be pointed out that Eq. (30) is still valid for the streams with $B>200$ m if the full mixing is completed across the channel. The discrepancy distribution of the predicted dispersion coefficient from the measured one for all the investigated streams is plotted in Fig. 6, where the discrepancy ratio is defined as $\log(K_P/K_M)$. Predictions with a large deviation from observed ones occur with quite a low frequency.

The longitudinal dispersion coefficients of the streams in Table 2 are also calculated from the widely used Fischer's equation (Fischer et al. 1979)

$$\frac{K_x}{HU^*}=0.011\left(\frac{B}{H}\right)^2\left(\frac{U}{U^*}\right)^2 \tag{50}$$

and from the empirical formula proposed by Seo and Cheong (1998)

$$\frac{K_x}{HU^*}=5.915\left(\frac{B}{H}\right)^{0.62}\left(\frac{U}{U^*}\right)^{1.428} \tag{51}$$

Eq. (51) was regarded to be superior in explaining dispersion characteristics of natural streams to existing equations (Seo and Cheong 1998). The calculated results from Eq. (50) are listed in the eighth column of Table 2. The dispersion coefficients predicted by the procedure presented in this paper and the ones computed from Eqs. (50) and (51) are compared with the measured ones in Fig. 7. The new method significantly improves the prediction of the longitudinal dispersion coefficient. It should be noted that all the curves in Figs. 1–8 should be smooth and continuous lines in theory.

The integration term in Eq. (30) contains the contribution from the lateral velocity deviation from the mean flow as well as the contribution from longitudinal gradients of the flow depth. By comparing the full integration with the integration of only the first term, the effect of the channel sinuosity is found. The ratio between $I_{\text{meandering}}$ and I_{straight} is shown in the tenth column of Table 2 for all the investigated streams. The ratio ranges from 1 to 85.4. It is clear that neglect of the effect of channel meandering causes large discrepancies between the predicted and observed dispersion coefficients. It is, therefore, essential to incorporate the effect of channel sinuosity in the theoretical equations to obtain a rea-

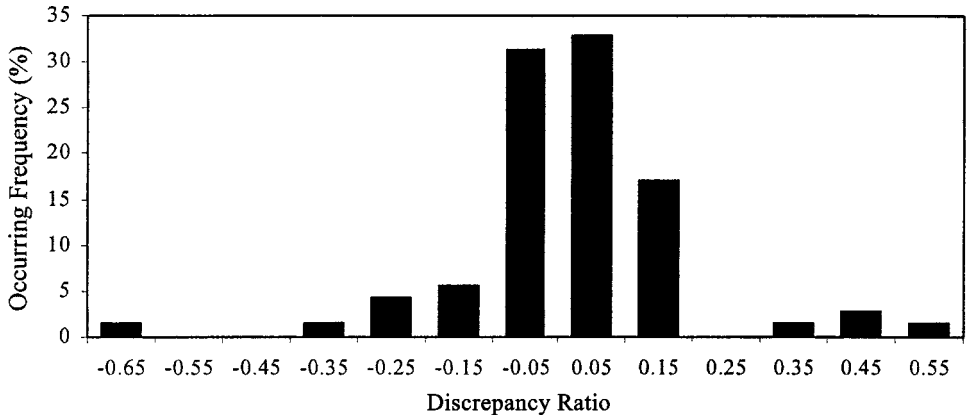

Fig. 6. Occurring frequency of discrepancy ratios predicted to measured K_x

sonable prediction of longitudinal dispersion coefficient. This is the distinct feature of the new method.

In principle, the proposed method is limited to the steady flow with constant cross-sectional averaged velocity U, flow depth H, and channel width B along a channel. Such conditions may rarely be satisfied strictly in natural streams but they may be met within certain length and time scales depending on the variability of a natural stream in terms of the accuracy of the proposed method and the observed data. Fig. 6 indicates that the discrepancies $\log(K_P/K_M)$ of this method mainly concentrate in the range of -0.15–0.15 or $0.708<K_P/K_M<1.412$, corresponding to $0.84<B/H<1.19$ or $0.84<U/U^*<1.19$ or $0.84<BU/(HU^*)<1.19$ in Eq. (30*c*). It means that 20% change in $(B/H)\times(U/U^*)$ is within the accuracy of the proposed method and the observed data and the length of a stream reach should be limited according to the 20% allowance in order to maintain a constant K_x. If a river reach is very long and it causes a greater change than the 20% allowance, then the river reach should be divided into several subreaches to meet the requirement of the proposed method.

Conclusions

Using the cross-sectional shape equation of straight channels, a more versatile channel shape or local flow depth equation is proposed for natural single channel streams by introducing the channel sinuosity, the dominating factor causing the significant variation in the longitudinal dispersion coefficient. Incorporating the effect of stream bends or the variation of local flow depth and hence the local velocity along the course of natural streams, a new triple integral expression of the longitudinal dispersion coefficient is derived. Then, an analytical method is developed for prediction of the longitudinal dispersion coefficient in natural streams by an approximation of the complex triple numerical integration with a set of regression equations for different width to depth ratios and sinuosity. The proposed procedure is verified by using 70 sets of field data collected from 30 streams from straight manmade canals to sinuous natural rivers in the United States. The new method predicts the longitudinal dispersion coefficient with an accuracy in which 91.4% of the calculated values range from 0.5 to 2 times the observed values. A comparison between the new method and other methods shows that the new method significantly improves the prediction of the longitudinal dispersion coefficient. The analytical method developed here can be applied with confidence to natural single-channel streams with the channel width of less than 200 m. The new analytical method is characterized by its capability of providing the most accurate pre

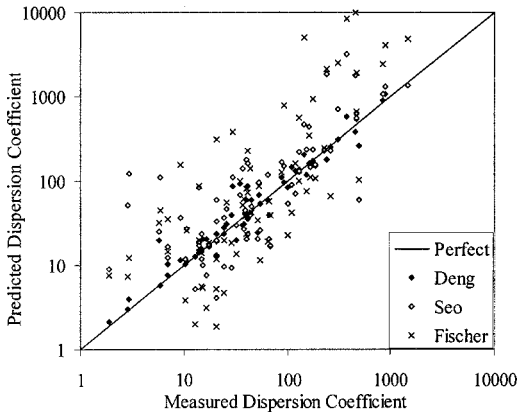

Fig. 7. Comparison between measured and predicted K_x

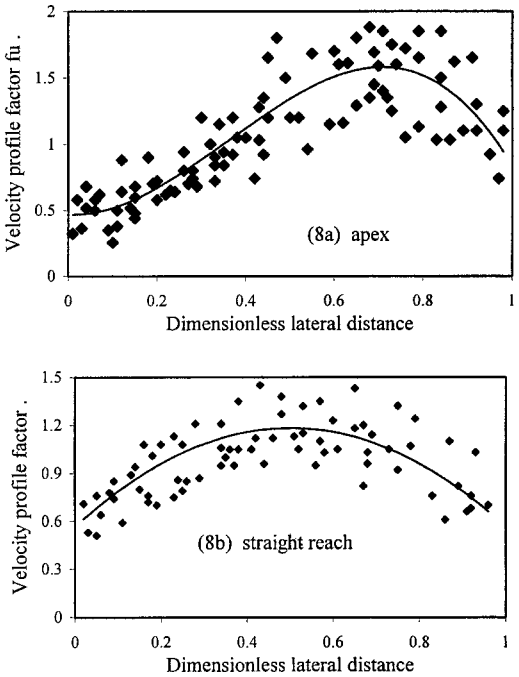

Fig. 8. Variation of velocity profile factor with ξ

diction of the longitudinal dispersion coefficient in single channel natural streams without detailed dye test concentration data as compared to existing other methods.

Appendix I. Integration over Flow Depth

As all the terms in Eq. (4) are continuous in the flow field the equation is thus integral over both the flow depth and the channel width and the order of differentiation and integration is interchangeable in terms of the Leibnitz rule. Inserting $\bar{u}=\bar{\bar{u}}+u''$, $\bar{v}=\bar{\bar{v}}+v''$, $\bar{w}=\bar{\bar{w}}+w''$, and $\bar{c}=\bar{\bar{c}}+c''$ into Eq. (4) and integrating the equation vertically from $z=0$ (channel bottom) to $z=h$ (water surface) by means of Leibnitz's rule for differentiation of integrals yields

$$\frac{\partial(h\bar{\bar{c}})}{\partial t}-\bar{\bar{c}}\frac{\partial h}{\partial t}+\frac{\partial(h\bar{\bar{u}}\bar{\bar{c}})}{\partial s}-(\bar{\bar{u}}\bar{\bar{c}})\frac{\partial h}{\partial s}+\frac{\partial(h\bar{\bar{v}}\bar{\bar{c}})}{\partial \eta}-(\bar{\bar{v}}\bar{\bar{c}})\frac{\partial h}{\partial \eta}+(\bar{\bar{w}}\bar{\bar{c}})_h$$
$$=\frac{\partial}{\partial s}\left(h(D_m+E_s)\frac{\partial \bar{\bar{c}}}{\partial s}\right)-\left((D_m+E_s)\frac{\partial \bar{\bar{c}}}{\partial s}\right)_h\frac{\partial h}{\partial s}+\frac{\partial}{\partial \eta}\left(h(D_m+E_\eta)\frac{\partial \bar{\bar{c}}}{\partial \eta}\right)-\left((D_m+E_\eta)\frac{\partial \bar{\bar{c}}}{\partial \eta}\right)_h\frac{\partial h}{\partial \eta}$$
$$-\left\{\frac{\partial}{\partial s}\left[\int_0^h(u''c'')dz\right]-(u''c'')_h\frac{\partial h}{\partial s}\right\}-\left\{\frac{\partial}{\partial \eta}\left[\int_0^h(v''c'')dz\right]-(v''c'')_h\frac{\partial h}{\partial \eta}\right\}-(w''c')_h \tag{52}$$

in which subscript h refers to the value at the water surface. After the integration the last term of Eq. (4) disappears because there is no mass flux to the atmosphere or through the bottom. The depth averaged c and uc are constant vertically and thus they occur without the subscript h after the integration. The terms $(u''c'')_h$, $(v''c'')_h$, and $(w''c'')_h$ are assumed to be much smaller than $\bar{\bar{u}}\bar{\bar{c}}$, $\bar{\bar{v}}\bar{\bar{c}}$, and $\bar{\bar{w}}\bar{\bar{c}}$, respectively.

Expressing the vertical integrations of $u''c''$ and $v''c''$ in the following form:

$$\int_0^h(u''c'')dz=h(\overline{u''c''})$$

and

$$\int_0^h(v''c'')dz=h(\overline{v''c''}) \tag{53}$$

As the turbulent intensity is usually regarded as zero at the water surface and the molecular diffusion coefficient D_m related terms are small at the water surface, Eq. (52) can be then recast as

$$\frac{\partial(h\bar{\bar{c}})}{\partial t}+\frac{\partial(h\bar{\bar{u}}\bar{\bar{c}})}{\partial s}+\frac{\partial(h\bar{\bar{v}}\bar{\bar{c}})}{\partial \eta}-\bar{\bar{c}}\left(\frac{\partial h}{\partial t}+\bar{\bar{u}}\frac{\partial h}{\partial s}+\bar{\bar{v}}\frac{\partial h}{\partial \eta}-\bar{\bar{w}}_h\right)$$
$$=\frac{\partial}{\partial s}\left(h(D_m+E_s)\frac{\partial \bar{\bar{c}}}{\partial s}\right)+\frac{\partial}{\partial \eta}\left(h(D_m+E_\eta)\frac{\partial \bar{\bar{c}}}{\partial \eta}\right)$$
$$-\frac{\partial h(\overline{u''c''})}{\partial s}-\frac{\partial h(\overline{v''c''})}{\partial \eta} \tag{54}$$

The fourth term on the left hand side of Eq. (54) is zero as

$$\frac{\partial h}{\partial t}+\bar{\bar{u}}\frac{\partial h}{\partial s}+\bar{\bar{v}}\frac{\partial h}{\partial \eta}-\bar{\bar{w}}_h=\frac{dh}{dt}-\bar{\bar{w}}_h=0 \tag{55}$$

In the case of the steady flow the vertical velocity $\bar{\bar{w}}_h$ at the water surface should be zero and thus $\bar{\bar{w}}_h=dh/dt=0$. The first three terms on the left hand side of Eq. (54) can be simplified as

$$\frac{\partial(h\bar{\bar{c}})}{\partial t}+\frac{\partial(h\bar{\bar{u}}\bar{\bar{c}})}{\partial s}+\frac{\partial(h\bar{\bar{v}}\bar{\bar{c}})}{\partial \eta}=h\frac{\partial \bar{\bar{c}}}{\partial t}+\bar{\bar{c}}\frac{\partial h}{\partial t}+h\frac{\partial(\bar{\bar{u}}\bar{\bar{c}})}{\partial s}+(\bar{\bar{u}}\bar{\bar{c}})\frac{\partial h}{\partial s}+h\frac{\partial(\bar{\bar{v}}\bar{\bar{c}})}{\partial \eta}+(\bar{\bar{v}}\bar{\bar{c}})\frac{\partial h}{\partial \eta}=h\left(\frac{\partial \bar{\bar{c}}}{\partial t}+\frac{\partial(\bar{\bar{u}}\bar{\bar{c}})}{\partial s}+\frac{\partial(\bar{\bar{v}}\bar{\bar{c}})}{\partial \eta}\right)+\bar{\bar{c}}\left(\frac{\partial h}{\partial t}+\bar{\bar{u}}\frac{\partial h}{\partial s}+\bar{\bar{v}}\frac{\partial h}{\partial \eta}\right)$$
$$=h\left(\frac{\partial \bar{\bar{c}}}{\partial t}+\frac{\partial(\bar{\bar{u}}\bar{\bar{c}})}{\partial s}+\frac{\partial(\bar{\bar{v}}\bar{\bar{c}})}{\partial \eta}\right)+\bar{\bar{c}}\frac{dh}{dt}=h\left(\frac{\partial \bar{\bar{c}}}{\partial t}+\frac{\partial(\bar{\bar{u}}\bar{\bar{c}})}{\partial s}+\frac{\partial(\bar{\bar{v}}\bar{\bar{c}})}{\partial \eta}\right) \tag{56}$$

Substitution of Eq. (56) into Eq. (54) leads to Eq. (5) in the main text.

Appendix II. Second Approach for *F*

u/U can be easily expressed in terms of the dimensionless depth and friction term based on the uniform-flow formulas mentioned before. For meandering rivers, u/U is often expressed in terms of the dimensionless depth and the dimensionless radius of curvature of the meandering channel (Chang 1988). In most of the dimensionless expressions of u/U, the dimensionless depth h/H is raised to a power of 0.5. Therefore, u/U is assumed to have the following general expression:

$$\frac{u}{U}=f_u\left(\frac{h}{H}\right)^{1/2}=f_u\left(\frac{h_*}{H_*}\right)^{1/2} \tag{57}$$

Table 3. Numerical Integration of Eq. (30)

	A	B	C	D	E	F	G	H	I	J	K	L	M	N	O	P	Q	R	S	T	U	V
1	ξ	$\bar{\xi}$	$\Delta\xi$	h_*	$h_*\Delta\xi$	H_*	$(h_*/H_*)^{0.7}$	Eq. (35)		First triple int		First triple int		I_*		Computation of the second triple integration in Eq. (47)						Eq. (30c)
2	0	0		0		0						0	0	0	0	0	0	0	0	0	0	187.70
3	0.025	0.0125	0.025	0.0005	1.165E−05	1.165E−05	0.00931	−1.2E−05	−1.16E-05	−30.8351	−30.835	0.0002	0.00018	0.0005	0.0005	−3.07E−7	−3.07E−7	−0.818	−0.818	4.7E−6	4.73036E−6	3.0175
4	0.050	0.0375	0.025	0.0055	0.000137	0.000149	0.04831	−0.0001	−0.00014	−0.86285	−31.698	0.0041	0.00432	0.0018	0.0024	−1.41E−5	1.44E−5	−0.817	−0.900	0.0001	0.00011845	1.710
5	0.075	0.0625	0.025	0.0166	0.000416	0.000566	0.10099	−0.0004	−0.00053	−0.23424	−31.932	0.0122	0.01648	0.0032	0.0056	−7.52E−5	−8.97E−5	−0.036	−0.936	0.0004	0.00046953	0.077
6	0.100	0.0875	0.025	0.0336	0.000839	0.001405	0.16118	−0.0007	−0.00126	−0.10795	−32.040	0.0234	0.03984	0.0046	0.0102	−0.0002	−0.0003	−0.024	−0.960	0.0007	0.00116202	62.204
7	0.125	0.1125	0.025	0.0555	0.001389	0.002794	0.22549	−0.0011	−0.00239	−0.06274	−32.103	0.0364	0.07630	0.0059	0.0161	−0.0004	−0.0007	−0.018	−0.978	0.0011	0.00226342	22.092
8	0.150	0.1375	0.025	0.0817	0.002043	0.004837	0.29172	−0.0016	−0.00396	−0.04156	−32.144	0.0502	0.12652	0.0071	0.0232	−0.0008	−0.0015	−0.015	−0.993	0.0015	0.00380413	2.021
9	0.175	0.1625	0.025	0.1113	0.002782	0.007619	0.35837	−0.0020	−0.00594	−0.02993	−32.174	0.0637	0.19018	0.0083	0.0316	−0.0012	−0.0027	−0.013	−1.005	0.0020	0.00578193	0.234
:	:	:	:	:	:	:	:	:	:	:	:	:	:	:	:	:	:	:	:	:	:	
22	0.500	0.4875	0.025	0.5911	0.014777	0.125463	1.09093	−0.0018	−0.04283	−0.00390	−32.303	0.0581	1.38036	0.0192	0.2233	−0.0075	−0.0649	−0.006	−1.107	0.0020	0.04492052	
23	0.525	0.5125	0.025	0.6314	0.015786	0.141249	1.14001	−0.0013	−0.04413	−0.00343	−32.307	0.0420	1.42231	0.0199	0.2432	−0.0078	−0.0727	−0.005	−1.112	0.0014	0.04636163	
:	:	:	:	:	:	:	:	:	:	:	:	:	:	:	:	:	:	:	:	:	:	
34	0.800	0.7875	0.025	1.0000	0.025000	0.378304	1.54891	0.00617	−0.01103	−0.00035	−32.323	−0.199	0.35246	0.0250	0.4980	−0.0060	−0.1580	−0.004	−1.159	−0.007	0.00837538	
35	0.825	0.8125	0.025	0.9936	0.024840	0.403144	1.54230	0.00600	−0.00503	−00020	−32.323	−0.194	0.15849	0.0249	0.5229	−0.0051	−0.1632	−0.004	−1.163	−0.007	0.00140617	
36	0.850	0.8375	0.025	0.9693	0.024233	0.427377	1.51706	0.00536	0.00033	−6.35E−05	−32.323	−0.173	−0.0148	0.0246	0.5475	−0.0042	−0.1674	−0.004	−1.168	−0.006	−0.0048437	
37	0.875	0.8625	0.025	0.9227	0.023067	0.450444	1.46801	0.00419	0.00452	7.43E−05	−32.323	−0.136	−0.1504	0.0240	0.5715	−0.0032	−0.1706	−0.005	−1.173	−0.005	−0.0097515	
38	0.900	0.8875	0.025	0.8486	0.021216	0.471660	1.38837	0.00250	0.00702	0.000218	−32.323	−0.081	−0.2310	0.0230	0.5946	−0.0023	−0.1729	−0.006	−1.179	−0.003	−0.0126880	
39	0.925	0.9125	0.025	0.7413	0.018532	0.490192	1.26869	0.00040	0.00742	0.000381	−32.323	−0.013	−0.2438	0.0215	0.6161	−0.0014	−0.1743	−0.009	−1.189	−0.000	−0.0131560	
40	0.950	0.9375	0.025	0.5941	0.014852	0.505044	1.09458	−0.0018	0.00565	0.000601	−32.322	0.0570	−0.1868	0.0193	0.6353	−0.0007	−0.1750	−0.016	−1.205	0.0021	−0.0110439	−0.000303
41	0.975	0.9625	0.025	0.3994	0.009986	0.515030	0.84008	−0.0032	0.00242	0.001001	−32.321	0.1045	−0.0823	0.0158	0.6511	−0.0002	−0.1752	−0.043	−1.248	0.0040	−0.0070794	−0.006686
42	1.000	0.9875	0.025	0.1490	0.003725	0.518755	0.43535	−0.0024	1.500E−16	0.003529	−32.318	0.0782	−0.00410	0.0097	0.6608	−1.32E−5	−0.1752	−0.511	−1.759	0.0036	−0.0034412	1459.3

where a velocity distribution factor f_u is introduced. Then, the dimensionless velocity deviation F can be determined as follows:

$$F=\frac{u}{U}-1=f_u\left(\frac{h_*}{H_*}\right)^{1/2}-1 \tag{58}$$

Actually, Eq. (58) can be obtained from Eq. (34) by taking the Chezy exponent. Based on the data measured on the bends of the Yangtze River, the largest river in China and collected by Zhang and Xie (1993), two regression equations of the velocity distribution factor $f_u(\xi)$ are obtained for the entrance and apex of the river bends

$$f_u(\xi)=-6.5565\xi^3+7.0775\xi^2-0.1579\xi+0.4704,$$

$$\text{for apex } R^2=0.7253 \tag{59a}$$

$$f_u(\xi)=-2.4682\xi^2+2.4682\xi+0.5658,$$

$$\text{for entrance or exit } R^2=0.5483 \tag{59b}$$

Eq. (59*a*), based on 96 sets of data, attains a maximum value $f_{u\,\max}=1.58$ at $\xi=0.708$, $f_u(0)=0.47$ at $\xi=0$, and $f_u(1)=0.837$ at $\xi=1$, as shown in Fig. 8(a). Eq. (59*b*), based on 72 sets of data, reaches a maximum value $f_{u\,\max}=1.18$ at $\xi=0.5$, $f_u(0)=0.5658$ at $\xi=0$, and $f_u(1)=0.5658$ at $\xi=1$, as shown in Fig. 8(b).

Appendix III. Engineering Application of Proposed Method

To demonstrate computation procedures of the numerical integration and interpolation, the geometrical and hydraulic properties of the Missouri River between the Sioux City, Iowa, and the Plattsmouth, Nebraska, are utilized. According to the dye test measurements in 1967 (Yotsukura et al. 1970), the best estimate of the longitudinal dispersion coefficient for the study reach from Blair Bridge to Plattsmouth Bridge is $K_x=16{,}000\ \text{ft}^2/\text{s}=1486.4\ \text{m}^2/\text{s}$, the average channel width $B=187.70$ m, the average flow depth $H=3.02$ m, the mean flow velocity $U=1.73$ m/s, and the mean shear velocity $U^*=0.0774$ m/s. These average hydraulic data come from Table 2 in the document by Yotsukura et al. (1970). Based on these mean values, the dimensionless transverse mixing coefficient M_* is calculated from Eq. (20*b*) as 2.02. The measured channel sinuosity $\sigma=1.44$ for the river reach from Blair to Plattsmouth. With these parameters known, the remaining unknown in Eq. (30*a*) is $I=I_0\times I_*$ to predict K_x. I_0 and I_* can be computed in Microsoft *Excel* following the procedures in Table 3 using Eqs. (47) and (42).

Column A: Dimensionless transverse coordinate $\xi=0.0-1.0$ with increment of 0.025.

Column B: The average $\bar{\xi}$ of two consecutive ξ values is obtained by setting $B3=(A3+A2)/2$ (It means that one writes the formula "$=(A3+A2)/2$" in the cell $B3$) and applying the formula to the whole column.

Column C: Increment $\Delta\xi$ of ξ is calculated by writing "$=A3\text{-}A2$" in the cell $C3$ or $C3=A3\text{-}A2$ and then applying the formula to the whole column.

Column D: Dimensionless flow depth h_* is calculated using its definition in Eq. (37) and the observed data by (1) setting $x=0$, (2) setting $D3=((B3)\text{^}(1.32))*(1\text{-}(1\text{-}2*(B3))\text{^}(4.1304))$ and applying the formula to the cells $D3-D22$ and $D23=((B23)\text{^}(1.32))*(1\text{-}(2*(B23)\text{-}1)\text{^}(4.1304))$ and applying it to the remaining cells in the column, (3) taking the maximum value 0.655346349 of h_* in the column as P in Eq. (37*a*), and (4) setting $D3=((B3)\text{^}(1.32))*(1\text{-}(1\text{-}2*(B3))\text{^}(4.1304))/0.655346349$ and applying the formula to cells $D3-D22$ and $D23=((B23)\text{^}(1.32))*(1\text{-}(2*(B23)\text{-}1)\text{^}(4.1304))/0.655346349$ and applying it to the remaining cells in the column, where the number 1.32 comes from $\alpha=3\times(1\text{-}0)\times(1.44\text{-}1)^1$ and 4.1304 stems from $\beta=\ln(B/H)=\ln(187.7/3.0175)=4.1304$ in Eq. (37).

Column E: Numbers in this column are obtained by setting $E3=(C3)*(D3)$ and applying it to the whole column.

Column F: Numbers in this column are obtained by setting $F3=F2+E3$ and applying it to the whole column. The last figure 0.518755213 ($F42$) in this column is the dimensionless mean depth H_*, i.e., $H_*=0.518755213$.

Column G: This column is to calculate the term $(h_*/H_*)^{2/3}$ in the triple integration. Numbers in this column are obtained by setting $G3=(D3/0.518755213)\text{^}(2/3)$ and applying it to the whole column.

Columns H and I: These two columns are used to find the correction factor ϕ satisfying Eq. (35) by adjusting the trial value of ϕ until the last figure (error) in cell $I42$ is less than 10^{-15} or so. The accuracy depends on $\Delta\xi$. The smaller the increment $\Delta\xi$, the smaller the error. $\phi=0.805023170076455$ causes an error of 1.50×10^{-16} in Eq. (35). Numbers in column H are finally obtained by setting $H3=(C3)*(D3)*(0.805023170076455*(G3)\text{-}1)$ and applying it to the whole column, and numbers in column I are obtained by setting $I3=I2+H3$ and applying it to the whole column.

Column J: Numbers in this column are obtained by setting $J3=((C3)*0.5*(I2+I3))/((D3)\text{^}(5/2))$ and applying it to the whole column. Here, the value 0.5 is to take on the average of I2 and I3.

Column K: Numbers in this column are obtained by setting $K3=K2+J3$ and applying it to the whole column.

Column L: Numbers in this column are obtained by setting $L3=((C3)*0.5*(K3+K2))*(D3)*(0.805023170076455*(G3)\text{-}1)$ and applying it to the whole column.

Column M: Numbers in this column are obtained by setting $M3=M2+L3$ and applying it to the whole column. The last value -0.00409809 ($M42$) in this column is the value of the first triple integration in Eq. (47).

Columns N and O: These two columns are used to calculate the parameter I_*. Numbers in column N are finally obtained by setting $N3=(C3)*((D3)\text{^}0.5)$ and applying it to the whole column. Numbers in column O are obtained by setting $O3=O2+N3$ and applying it to the whole column. The last figure 0.660799 ($O42$) in this column is the value of I_* in Eq. (30), i.e., $I_*=0.660799$.

Column P: Numbers in this column are obtained by setting $P3=(C3)*(LN(B3))*((D3)\text{^}(5/3))$ and applying it to the whole column.

Column Q: Numbers in this column are obtained by setting $Q3=Q2+P3$ and applying it to the whole column.

Column R: Numbers in this column are obtained by setting $R3=((C3)*0.5*(Q2+Q3))/((D3)\text{^}(5/2))$ and applying it to the whole column.

Column S: Numbers in this column are obtained by setting $S3=S2+R3$ and applying it to the whole column.

Column T: Numbers in this column are obtained by setting $T3=((C3)*0.5*(S2+S3))*(D3)*(0.805023170076455*(G3)\text{-}1)$ and applying it to the whole column.

Column U: Numbers in this column are obtained by setting $U3=U2+T3$ and applying it to the whole column. The last value -0.003441201 ($U42$) in this column is the value of the

second triple integration without the coefficient in Eq. (47).

Column V: The last column is to calculate the longitudinal dispersion coefficient K_x using the available hydraulic data, where cell $V2$ is B, $V3$ is H, $V4$ is U, and $V5$ is U^*, $V6 = V2/V3$, $V7 = V4/V5$, $V8 = 0.145 + ((V6)\text{^}1.38)*(V7)/3520$, $V9 = (V3)*(V5)$. $V40$ is calculated by setting $V40 = -0.0013/((V6)\text{^}0.3523)$, that gives the I value at $x = L$ or for $\sigma = 1$. Actually, in the case of $x = L$ or $\sigma = 1$ the I value can be calculated following the same procedure as mentioned above for the case of $x = 0$. Cell $V41$ gives the average I value of a river reach including at least one bend and one straight transition portion by setting $V41 = ((6*(0.44\text{^}1)*(0.805023170076455*(U42)/((F42)\text{^}(2/3))) + M42)*(O42) + V40)/1.57$. This formula can be interpreted as the average $I = (I_{x=0} + I_{x=L})/1.57$, where $I = I_0 I_*$. The number in the cell $V42$ is obtained from Eq. (30c) by setting $V42 = -(V41)*((V6)\text{^}(2))*((V7)\text{^}2)*(V9)/(V8)$. It finally gives the predicted longitudinal dispersion coefficient of the Missouri River between the Blair Bridge to the Plattsmouth Bridge, i.e., $K_x = 1459.3$ m^2/s, close to the observed value of 1486.4 m^2/s.

The value of I can also be calculated using the regression equations in Table 1 and interpolation method. For the investigated reach of the Missouri River, $4 < \beta = 4.1304 < 5$. Substitution of $\sigma = 1.44$ into the last two equations in Table 1 yields $I(\beta = 4) = 0.00605$ and $I(\beta = 5) = 0.00726$. Linear interpolation of the two I values gives $I(\beta = 4.1304) = 0.1304 \times (0.00726 - 0.00605) + 0.00605 = 0.00621$, leading to $K_x = 1355.4$ m^2/s. It is apparent that the methods proposed in this paper are capable of predicting the longitudinal dispersion coefficient of natural streams with high accuracy as long as the observed hydraulic and geometrical data are accurate. Table 1 in conjunction with the interpolating method is suggested for engineers to calculate I values and then K_x as it can give a simple yet reasonably accurate prediction of K_x.

Notation

The following symbols are used in this paper:

A = cross-sectional area of river channel (m^2);
a = generalized friction factor;
B = surface width of river channel (m);
b = exponent of flow depth in generalized local velocity equation;
C = cross-sectional average concentration;
C' = deviation of local depth mean concentration from cross-sectional mean;
C_0 = cross-sectional average concentration at $x = 0$;
c = instantaneous concentration;
$\bar{c}$ = time-averaged concentration;
c' = turbulent fluctuating concentration;
$\bar{\bar{c}}$ = depth-averaged concentration;
c'' = deviation of $\bar{c}$ from $\bar{\bar{c}}$;
D = molecular diffusion coefficient (m^2/s);
E = turbulent diffusion coefficient (m^2/s);
F = deviation of dimensionless local depth mean velocity from cross-sectional mean;
f_u = velocity distribution factor;
H = sectional average flow depth (m);
H_* = sectional averaged dimensionless flow depth;
h = local flow depth (m);
$h_{\max}$ = maximum flow depth (m);
h_* = dimensionless flow depth;
I = revised triple integration by I_*;
I_0 = triple integration;
I_* = correction factor of shear velocity for replacement of hydraulic radius by local flow depth;
K_M = measured longitudinal dispersion coefficient (m^2/s);
K_P = predicted longitudinal dispersion coefficient (m^2/s);
K_{sz} = dispersion coefficient in s direction due to vertical gradients of $\bar{u}$ and $\bar{c}$;
K_x = longitudinal dispersion coefficient (m^2/s);
K_{x0} = longitudinal dispersion coefficient in straight stream (m^2/s);
$K_{\eta z}$ = dispersion coefficient in η direction due to vertical gradients of $\bar{v}$ and $\bar{c}$;
L = distance from bend apex to exit measured along meander path (m);
L_{m} = meander wave length (m);
M_{y} = transverse mixing coefficient (m^2/s);
M_* = dimensionless transverse mixing coefficient;
n = Manning roughness coefficient;
P = maximum value of p;
p = dimensionless local flow depth;
R = hydraulic radius (m);
S = channel slope;
s = longitudinal coordinate;
t = time;
U = cross-sectional averaged longitudinal velocity (m/s);
U' = deviation of local depth mean velocity from cross-sectional mean (m/s);
U^* = cross-sectional shear velocity (m/s);
u^* = local shear velocity (m/s);
$u^*_{\max}$ = maximum shear velocity (m/s);
u,v,w = instantaneous velocities in s, η, and z directions (m/s);
$\bar{u},\bar{v},\bar{w}$ = time-averaged velocities in s, η, and z directions (m/s);
$\bar{\bar{u}},\bar{\bar{v}},\bar{\bar{w}}$ = depth-averaged velocities in s, η, and z directions (m/s);
u',v',w' = turbulent fluctuating velocities in s, η, and z directions (m/s);
u'',v'',w'' = deviations of $\bar{u}$, $\bar{v}$, $\bar{w}$ from $\bar{\bar{u}}$, $\bar{\bar{v}}$, $\bar{\bar{w}}$, respectively (m/s);
x = longitudinal coordinate along meander path;
y = lateral coordinate;
z = vertical coordinate;
α = skewness parameter of channel cross section;
β = channel shape parameter;
γ = correction factor;
δ = numerical constant;
η = lateral coordinate;
θ = correction factor;
ξ = dimensionless transverse distance y/B;
π = 3.14159 . . . .
σ = channel sinuosity;
ϕ = correction factor; and
ψ = correction factor.

References

Bencala, K. E., and Walters, R. A. (1983). "Simulation of solute transport in a mountain pool-and-riffle stream: a transient storage model." *Water Resour. Res.,* 19(3), 718–724.

Chang, H. H. (1988). *Fluvial processes in river engineering*, Wiley, New York, 10–27, 306–309.

Chatwin, P. C. (1971). "On the interpretation of some longitudinal dispersion experiments." *J. Fluid Mech.,* 48(4), 689–702.

Chow, V. T. (1959). *Open-channel hydraulics*, McGraw-Hill, New York, 26–27, 98–125.

Czernuszenko, W. (1990). "Dispersion of pollutants in flowing surface waters." *Encyclopedia of fluid mechanics*, Gulf, Houston, 119–169.

Czernuszenko, W., and Rowinski, P. M. (1997). "Properties of the dead-zone model of longitudinal dispersion in rivers." *J. Hydraul. Res.,* 35(4), 491–504.

Czernuszenko, W., Rowinski, P. M., and Sukhodolov, A. (1998). "Experimental and numerical validation of the dead-zone model for longitudinal dispersion in rivers." *J. Hydraul. Res.,* 36(2), 269–280.

Deng, Z.-Q., and Singh, V. P. (1999). "Mechanism and conditions for change in channel pattern." *J. Hydraul. Res.,* 37(4), 465–478.

Deng, Z.-Q., Singh, V. P., and Bengtsson, L. (2001). "Longitudinal dispersion coefficient in straight rivers." *J. Hydraul. Eng.,* 127(11), 919–927.

Elder, J. W. (1959). "The dispersion of a marked fluid in turbulent shear flow." *J. Fluid Mech.,* 5(4), 544–560.

Fernald, A. G., Wigington, Jr., P. J., and Landers, D. H. (2001). "Transient storage and hyporheic flow along the Willamette River, Oregon: field measurements and model estimates." *Water Resour. Res.,* 37(6), 1681–1694.

Fischer, B. H. (1967). "The mechanics of dispersion in natural streams." *J. Hydraul. Div., Am. Soc. Civ. Eng.,* 93(6), 187–216.

Fischer, H. B. (1969). "The effect of bends on dispersion in streams." *Water Resour. Res.,* 5(2), 496–506.

Fischer, H. B., List, E. J., Koh, R. C. Y., Imberger, J., and Brooks, N. H. (1979). *Mixing in inland and coastal waters*, Academic. New York, 104–138.

Godfrey, R. G., and Fredrick, B. J. (1970). "Stream dispersion at selected sites." *Professional Rep. No. 433-K*, U.S. Geological Survey.

Holley, E. R. (1969). "Unified view of diffusion and dispersion." *J. Hydraul. Div., Am. Soc. Civ. Eng.,* 95(2), 621–631.

Lau, Y. L., and Krishnappan, B. G. (1981). "Modeling transverse mixing in natural streams." *J. Hydraul. Div., Am. Soc. Civ. Eng.,* 107(2), 209–226.

Lees, J. M., Camacho, L. A., and Chapra, S. (2000). "On the relationship of transient storage and aggregated dead zone models of longitudinal solute transport in streams." *Water Resour. Res.,* 36(1), 213–224.

Liu, H. (1977). "Predicting dispersion coefficient of streams." *J. Environ. Eng. Div., Am. Soc. Civ. Eng.,* 103(1), 59–69.

Martin, J. L., and McCutcheon, S. C. (1999). *Hydrodynamics and transport for water quality modeling*, CRC, Boca Raton, Fla., 7–220.

McCutcheon, S. C. (1989). *Water quality modeling*, Vol. I, CRC, Boca Raton, Fla., 27–171.

McQuivey, R. S., and Keefer, T. N. (1974). "Simple method for predicting dispersion in streams." *J. Environ. Eng. Div., Am. Soc. Civ. Eng.,* 100(4), 997–1011.

McQuivey, R. S., and Keefer, T. N. (1976). "Dispersion–Mississippi River below Baton Rouge, La." *J. Hydraul. Div., Am. Soc. Civ. Eng.,* 102(10), 1425–1437.

Nordin, C. F., and Sabol, G. V. (1974). "Empirical data on longitudinal dispersion in rivers." *Water Resources Investigations Rep. No. 20–74*, U.S. Geological Survey.

Piasecki, M., and Katopodes, N. D. (1999). "Identification of stream dispersion coefficients by adjoint sensitivity method." *J. Hydraul. Eng.,* 125(7), 714–724.

Przedwojski, B., Blazejewski, R., and Pilarczyk, K. W. (1995). *River training techniques: fundamentals, design and applications*. A. A. Balkema, Rotterdam, The Netherlands, 302–319.

Rutherford, J. C. (1994). *River mixing*, Wiley, Chichester, U.K., 102–200.

Schumm, S. A. (1963). "Sinuosity of alluvial rivers on the Great Plains." *Geol. Soc. Am. Bull.,* 74, 1089–1100.

Seo, I. W., and Cheong, T. S. (1998). "Predicting longitudinal dispersion coefficient in natural streams." *J. Hydraul. Eng.,* 124(1), 25–32.

Seo, I. W., and Cheong, T. S. (2001). "Moment-based calculation of parameters for the storage zone model for river dispersion." *J. Hydraul. Eng.,* 127(6), 453–465.

Sooky, A. A. (1969). "Longitudinal dispersion in open channels." *J. Hydraul. Div., Am. Soc. Civ. Eng.,* 95(4), 1327–1346.

Taylor, G. I. (1953). "Dispersion of soluble matter in solvent flowing slowly through a tube." *Proc. R. Soc. London, Ser. A,* 219, 186–203.

Taylor, G. I. (1954). "The dispersion of matter in turbulent flow through a pipe." *Proc. R. Soc. London, Ser. A,* 223, 446–468.

Wörman, A. (2000). "Comparison of models for transient storage of solutes in small streams." *Water Resour. Res.,* 36(2), 455–468.

Yotsukura, N., Fischer, H. B., and Sayre, W. W. (1970). "Measurement of mixing characteristics of the Missouri River between Sioux City, Iowa, and Plattsmouth, Nebraska." *Water-Supply Rep. No. 1899-G*, U.S. Geological Survey.

Zhang, R. J., and Xie, J. H. (1993). *Sedimentation research in China*, China Water and Power Press, Beijing, 228–229.